Development 130, 2981-2996

doi:10.1242/dev.00496

Somatic motoneurone specification in the hindbrain: the influence of somite-derived signals, retinoic acid and Hoxa3

Sonia Guidato[1], Fabrice Prin and Sarah Guthrie*

MRC Centre for Developmental Neurobiology, 4th Floor New Hunt's House, King's College, Guy's Campus, London SE1 1UL, UK
[1]Present address: Department of Developmental Neurobiology, National Institute for Medical Research, The Ridgeway, Mill Hill, London NW7 1AA, UK
*Author for correspondence (e-mail: sarah.guthrie@kcl.ac.uk)

Accepted 18 March 2003

SUMMARY

We have investigated the mechanisms involved in generating hindbrain motoneurone subtypes, focusing on somatic motoneurones, which are confined to the caudal hindbrain within rhombomeres 5-8. Following heterotopic transplantation of rhombomeres along the rostrocaudal axis at various developmental stages, we have found that the capacity of rhombomeres to generate somatic motoneurones is labile at the neural plate stage but becomes fixed just after neural tube closure, at stage 10-11. Grafting of somites or retinoic acid-loaded beads beneath the rostral hindbrain induced the formation of somatic motoneurones in rhombomere 4 only, and Hox genes normally expressed more caudally (*Hoxa3, Hoxd4*) were induced in this region. Targeted overexpression of *Hoxa3* in the rostral hindbrain led to the generation of ectopic somatic motoneurones in ventral rhombomeres 1-4, and was accompanied by the repression of the dorsoventral patterning gene *Irx3*. Taken together, these observations suggest that the somites, retinoic acid and Hox genes play a role in patterning somatic motoneurones in vivo.

Key words: Somatic motoneurones, Rostrocaudal axis, Hindbrain, Retinoic acid, Hox genes, Somites, Quail, Chick

INTRODUCTION

During the development of the vertebrate nervous system, the fate adopted by each progenitor cell depends on its position along the rostrocaudal and dorsoventral axes of the neural tube, and on extrinsic signals and intrinsic gene expression. Some of these specification steps have been elucidated for motoneurones, which develop in the ventral neural tube and comprise a number of sub-populations. The early differentiation of motoneurones is known to depend on sonic hedgehog (Shh)-mediated signals which are transmitted from the notochord and the floor plate ventrodorsally across the neuroepithelium (reviewed by Tanabe and Jessell, 1996). Shh-mediated signalling leads to the expression of a key set of transcription factors within distinct dorsoventral progenitor domains, each of which generates a distinct class of neurones, including motoneurones (Briscoe et al., 2000; Jessell, 2000).

Motoneurones later diversify into subpopulations that form discontinous columns, occupying distinct domains along the rostrocaudal axis. In the cranial region, motoneurones are subdivided into branchiomotor (BM), visceral motor (VM) and somatic motor (SM) neurone subtypes, depending on their columnar organisation and synaptic target. These subpopulations are thought to originate within particular dorsoventral progenitor domains. For example, BM/VM neurones are born in a domain immediately dorsal to the floor plate, which expresses *Nkx2.2*, whereas SM neurones originate in a domain dorsal to this, which is *Nkx2.2*-negative but which expresses *Pax6* at low levels and *Olig2* (Briscoe et al., 1999; Briscoe et al., 2000; Novitch et al., 2001; Jessell, 2000).

Patterning of motoneurones along the rostrocaudal axis may depend on signals from the paraxial mesoderm because, in the trunk region, heterotopic transplantation of the paraxial mesoderm can alter some aspects of motoneurone phenotype (Ensini et al., 1998; Matise and Lance-Jones, 1996). Retinoic acid (RA), fibroblast growth factors (FGFs) and the TGFβ family member GDF11 have also been implicated in conferring rostrocaudal identity on spinal motoneurones (Liu et al., 2001; Sockanathan and Jessell, 1998). The actions of these, and possibly other mesoderm-derived molecules, appear to repattern the rostrocaudal expression domains of Hoxc genes, which are expressed in discrete rostrocaudal domains of the neural tube (Ensini et al., 1998; Liu et al., 2001), conferring upon Hox genes a central role in the interpretation of extrinsic signals in motoneurone patterning.

In the hindbrain, motoneurone patterning is linked to segmentation into rhombomeres, each of which contains a characteristic set of motoneurone subtypes with distinct axon pathways. BM, VM and SM neurone subtypes are differentially distributed with respect to the rostrocaudal axis: rhombomeres 2-4 contain only BM neurones (Lumsden and Keynes, 1989), whereas rhombomeres 5-8 contain BM, VM and SM neurones in various combinations. Segmentation occurs between stage 9 and stage 12 in the chick embryo, but

a coarse rostrocaudal pattern is established even earlier, at neural plate stages, providing a substrate upon which later dorsoventral patterning acts (Lumsden and Krumlauf, 1996; Simon et al., 1995). Rhombomeres express different combinations of Hox genes, which play roles in segmentation, rhombomere patterning and neuronal differentiation (Lumsden and Krumlauf, 1996). In particular, some Hox genes, including *Hoxb1*, are expressed at early neural plate stages and it is plausible that they might act to establish rhombomeres as territories committed to generate particular repertoires of motoneurones. Recently, *Hoxb1* and *Hoxa2* have been shown to play a direct role in the specification of facial and trigeminal motoneurones, respectively (Gavalas et al., 1997; Bell et al., 1999; Jungbluth et al., 1999; Studer et al., 1996).

As in the spinal cord, patterns of Hox gene expression are responsive to environmental signals, including those from the mesoderm. Transposition of rhombomeres from the pre-otic region to the post-otic region at stage 10-12 resulted in respecification of the Hox 'code' and neuronal organisation (Grapin-Botton et al., 1995; Itasaki et al., 1996), whereas transpositions of rhombomeres between axial levels within the pre-otic region resulted in the maintenance of rhombomere identity and Hox gene expression (Grapin-Botton et al., 1997; Grapin-Botton et al., 1995; Guthrie et al., 1992; Itasaki et al., 1996; Kuratani and Eichele, 1993). The discrepancy seems to depend on differences in the paraxial mesoderm, which is unsegmented in the pre-otic region (Hacker and Guthrie, 1998), but forms somites caudal to the otic vesicle. Somite grafts adjacent to the neural tube in the pre-otic region were capable of respecifying Hox gene expression and some aspects of neuronal phenotype, effects that could be mimicked by RA (Gavalas and Krumlauf, 2000; Gould et al., 1998; Grapin-Botton et al., 1997; Grapin-Botton et al., 1995; Itasaki et al., 1996). RA is known to be produced by the somites, making it a likely candidate for a caudalising signal in vivo (Maden et al., 1998; Swindell et al., 1999). An in vivo role of RA has been demonstrated in a series of studies on avian and mouse embryos, in which depletion or elimination of RA signalling leads to a failure in the development of rhombomeres 4-7 (Dupé and Lumsden, 2001; Gale et al., 1999; Maden, 1996; Niederreither et al., 2000).

However, in these studies, only selected aspects of rhombomere identity were examined and these did not include cranial motoneurone identities or axon trajectories. No systematic study has been carried out to elucidate the precise relationship between environmental signals, patterns of Hox gene expression and motoneurone specification. It is not clear at which timepoint rhombomeres become committed to generating particular motoneurone subtypes, nor is the source and nature of the inductive signals that control these processes known. In the present work we focus on these issues, and investigate in particular the mechanisms that govern somatic motoneurone generation in the hindbrain and confine it to caudal rhombomeres (5-8). We have performed transplantation experiments in early chick embryos, which indicate that the capacity of a rhombomere to generate SM neurones is labile at the neural plate stage but becomes fixed at stage 10-11, around the time of neural tube closure. Somites grafted rostrally were able to induce ectopic Hox gene expression (including that of *Hoxa3*) and SM neurones, in particular rhombomeres, in a restricted time period. RA-loaded beads grafted rostrally mimicked this effect, inducing SM neurones in the same region and within the same time window. We also tested a possible involvement of *Hoxa3* in defining the territory that generates SM neurones, and found that ectopic expression of *Hoxa3* in the rostral hindbrain induced SM neurones in rostral rhombomeres.

MATERIALS AND METHODS

Transplantation experiments, somite and RA bead grafting

Stage 9-12 embryos were used in stage-matched quail-to-chick or bead grafting experiments. For all microsurgery, host eggs were windowed and embryos made visible by sub-blastodermal injection of India ink (1:20 dilution in Howard's Ringer Solution). Surviving embryos were harvested at embryonic day 6 [E6: HH stage 26-29 (Hamburger and Hamilton, 1951)], when heads were removed and fixed in 3.5% paraformaldehyde (PFA) for 2 hours before in situ hybridisation or immunohistochemistry. Operations were performed as previously described (Guthrie et al., 1992). Somites for grafting were dissected from quail donors and grouped in a caudal population [caudal to and including somite 5 (s5)] and a rostral population (s1 to s3 only). For RA bead grafts, AG 1-X2 resin (Bio-Rad, 143-1255) was washed in phosphate buffered saline (PBS), incubated in the dark at room temperature for 1 hour in PBS containing all trans-RA (Sigma, R2625; 1×10^{-4} M or 5×10^{-4} M) and finally washed again in PBS. Individual somites or beads were then grafted into isochronic chick hosts at various levels within the cranial paraxial mesoderm and beneath the neuroepithelium. Beads were washed in PBS prior to grafting.

Rhombomere fate mapping

Because rhombomere boundaries are not complete until stage 12 (Vaage, 1969), the territories corresponding with presumptive rhombomeres were mapped in both chick and quail embryos at stage 9. Small spots of DiI (Molecular Probes, Oregon, USA) were injected, using a micrometer graticule, at defined positions within the neural tube, relative to a caudal limit at the first somite and the rostral end of the neural tube. Embryos were incubated for 24 hours prior to analysis. Rhombomere 1 (r1) was mapped at 900 μm from the rostral end of the neural tube, and thereafter each rhombomere was approximately 100 μm long, with r7 located at level of the first somite. These measurements were used to ensure accurate dissection of rhombomeres for transplantation.

In ovo electroporation of chick embryos

In the electroporation experiments, we used full-length cDNA for *tauGFP* (green fluorescent protein), mouse *Hoxa3* and human *HOXB3* (gifts from Dr Andrea Brand, Dr Michael Hofmann and Dr Guy Sauvageau, respectively) under the control of a chicken β-actin promoter (pCAβlink kindly provided by Dr Jon Gilthorpe). The *tauGFP* plasmid was co-electroporated with the mouse *Hoxa3* or human *HOXB3* plasmid to allow in vivo fluorescent screening of embryos. We found that a 1:3 ratio of *tauGFP/Hoxa3* or *HOXB3* gave the best co-localization of *GFP* and Hox gene expression. Plasmids were used at a combined final concentration of 2 μg/μl, whereas in control experiments the *tauGFP* plasmid alone was used at a final concentration of 0.5 μg/μl. Electroporation was performed as previously described (Itasaki et al., 1999). Briefly, eggs were windowed and embryos (stage 8-17) made visible. The vitelline membrane was opened and DNA solution was injected either into the neural tube (stage 9-17) or on top of the neural plate (stage 8). Two silver electrodes were then placed dorsal and ventral to the embryo at the rostrocaudal level desired, so that electroporation (10V; 5 pulses of 50 milliseconds) allowed the entry of DNA into the basal plate of the neural tube where motoneurone progenitors are located. Unilateral entry of DNA was obtained in most cases. Eggs were then sealed and

incubated for 48-96 hours before embryos were removed for fixation (at E4-E6).

In situ hybridisation

Whole-mount in situ hybridisation was performed essentially as published (Henrique et al., 1995), using *Islet2* (Tsuchida et al., 1994), *Hb9* (Tanabe et al., 1998), *Hoxa3* (Saldivar et al., 1996), *Hoxb3* (Rex and Scotting, 1994) and *Hoxd4* (Grapin-Botton et al., 1995) chick-specific probes. A mouse *Hoxa3* probe (full-length cDNA; GenBank Accession Number Y11717) was used to detect the expression of electroporated *Hoxa3*. Briefly, stage 28-30 embryos were fixed, dehydrated in methanol and stored at –20°C for a maximum of 2 weeks. Prior to pre-hybridisation and hybridisation at 70°C, embryos were treated with 10 μg/ml proteinase K for 20 minutes at room temperature. Digoxigenin (DIG)- or Fluorescein (Fluo)-labelled antisense RNA probes were synthesised according to the manufacturer's instructions (Roche Molecular Biochemicals), and hybridised at 1 μg/ml. For double in situ hybridisation, probes were added simultaneously to the embryos, whereas antibody incubations (anti-DIG-AP and anti-Fluo-AP antibodies) and developing reactions were carried out sequentially. The NBT/BCIP reaction was always performed first, followed by a series of washes and a 30 minute incubation at 70°C to destroy residual alkaline phosphatase activity. Incubation with the anti-Fluo-AP antibody and Fast Red development followed. All reagents used for in situ procedures were from Roche Molecular Biochemicals, except for Fast Red (Sigma).

Immunostaining on whole mounts in rhombomere and somite grafting experiments

In grafting experiments, the correct graft position and integration was ensured by immunostaining with a monoclonal antibody to quail cells (QCPN). Following the in situ procedure, embryos were post-fixed, washed extensively in PBS containing 1% Triton X-100 (TX100), and left in blocking solution (PBS/10% heat-inactivated sheep serum (HSS)/1% TX100) for a minimum of 2 days prior to incubation with the primary antibody. After 2-3 days, embryos were washed extensively in PBS/10% HSS/1% TX100, incubated for further 2-3 days in secondary antibody, then finally washed overnight, dissected and mounted in DABCO/glycerol.

Immunohistochemistry on sections

Cryostat sections (10 μm) were immunostained by overnight incubation with primary antibodies in PBS/1% HSS/0.1% TX100. After several washes in PBS/0.02% TX100, sections were incubated for 2-3 hours at room temperature with fluorescent-conjugated secondary antibodies (FITC-, Cy3-, Alexa Fluor 568- or Cy5-labelled goat anti-mouse, goat anti-guinea pig or goat anti-rabbit antibodies), washed briefly and mounted in DABCO/glycerol prior to analysis. Vibratome sections (80 μm) were incubated with primary antibodies for 2 days in PBS/10% HSS/1% TX100. Sections were then washed extensively in PBS/1% TX100 and incubated overnight with secondary antibodies. After final washes, sections were mounted in DABCO/glycerol.

Primary antibodies used were polyclonal anti-neurofilament heavy chain (AB1991, Chemicon International), monoclonal anti-quail axons or quail cells (QN or QCPN, respectively; Developmental Studies Hybridoma Bank), monoclonals 4D5 (anti-Islet1/2), 4H9 (anti-Islet2), and polyclonals anti-Chx10 and anti-Lim3 (all kind gifts of Dr T. Jessell). We also used monoclonals anti-Nkx2.2, 81C10 (anti-Mnr2/Hb9) and anti-Pax6, and polyclonals anti-Irx3 and anti-Olig2 (also kind gifts of Dr T. Jessell). Finally in misexpression experiments, a rabbit anti-GFP antibody (A-6455, Molecular Probes) was used to identify electroporated regions. All fluorescently-conjugated secondary antibodies were from Jackson ImmunoResearch Laboratories, except for Alexa Fluor 568, which was from Molecular Probes.

RESULTS

Motoneurone organisation and gene expression patterns in the chick hindbrain

Cranial motor nuclei are located at distinct positions along the rostrocaudal axis of the hindbrain, and may contain one or more of BM, VM and SM neuronal subtypes (Fig. 1A). Whereas BM and VM axons exit the neuroepithelium via large, single exit points, SM axons exit ventrally in small groups. Rhombomeres 2-4 (r2-4) contain only BM neurones and a small population of vestibulo-acoustic neurones (Lumsden and Keynes, 1989; Simon and Lumsden, 1993), whereas r5-8 contains BM, VM and SM neurones in various combinations. The trigeminal (V; r2 and r3) and cranial accessory (XI; r7 and r8) nuclei contain only BM neurones, whereas the facial (VII; r4 and r5), glossopharyngeal (IX; r6 and r7) and vagus (X; r7 and r8) nuclei contain BM and VM neurones. SM neurones are found in the oculomotor (III; midbrain), and trochlear (IV; r1), abducens (VI; r5 and 6) and hypoglossal (XII; r7 and 8) nuclei (Fig. 1A).

Whereas all cranial motoneurones express the Lim homeobox gene *Islet1*, SM neurones co-express *Islet2* and/or *Lim3* genes (Fig. 1A,B) (Varela-Echavarría et al., 1996). *Lim3* is expressed in the dividing progenitors of all SM neurones, but its expression is maintained only in subsets of post-mitotic hypoglossal and abducens SM neurones (Sharma et al., 1998; Varela-Echavarría et al., 1996). Hypoglossal neurones express *Islet1*, *Islet2* and *Lim3*, and at E6 a substantial subpopulation co-expresses *Islet2* and *Lim3*. Neurones of the main abducens nucleus in r5 and r6 express *Islet1* and *Islet2*, whereas those of the small accessory abducens nucleus in r5 migrate laterally, switch off *Islet2*, and thereafter express *Islet1* and *Lim3* (Varela-Echavarría et al., 1996) (data not shown). For this reason, abducens and hypoglossal neurones can be distinguished based on the co-expression of *Islet2/Lim3* by the latter, but not the former, population. The homeobox-containing gene *Hb9* is expressed by post-mitotic SM neurones of both the abducens and hypoglossal nuclei (Fig. 1A,C) (Pfaff et al., 1996; Tanabe et al., 1998). The two other groups of SM neurones (oculomotor nucleus in the midbrain and trochlear nucleus in rostral r1) do not express *Hb9* (Fig. 1C). In the chick, *Hb9* and *Islet2* are first expressed in hindbrain SM neurones at stages 16 and 22, respectively, whereas *Lim3* expression is initiated in post-mitotic neurones at around stage 25 (Varela-Echavarría et al., 1996). Thus, none of the markers are expressed at the time of grafting (stage 9-12), allowing us to test the commitment of rhombomeres to express these genes.

Both in chick and mouse embryos, Hox3 paralogues have been reported to be expressed from the r4/5 boundary caudally (Grapin-Botton et al., 1995; Lumsden and Krumlauf, 1996; Rex and Scotting, 1994). However, although this was the expression pattern of *Hoxa3* in the chick (Fig. 1D), we found that, at E6, *Hoxb3* was also expressed in r4, with a rostral cut-off at the r3/4 boundary (Fig. 1A,E). Double in situ hybridisation for *Hoxb3* and *Islet2* confirmed this localisation, because the abducens neurones of r5 and r6 were completely contained within the *Hoxb3*-expressing territory (Fig. 1E). *Hoxd4* was expressed from the r6/7 boundary caudally, in accordance with previous reports (Grapin-Botton et al., 1995), and double in situ hybridisation with *Hoxd4* and *Islet2* showed that hypoglossal neurones lay within the *Hoxd4*-expressing

domain, whereas abducens neurones lay rostral to this region (Fig. 1F). Thus *Hoxa3*, *Hoxb3* and *Hoxd4* were used as markers of more caudal rhombomere identity.

In pre-otic rhombomere transplants, Lim gene expression and motoneurone identity is fixed from stage 10 onward

To ascertain the timing of rhombomere commitment to generate SM neurones, r5 to r3 (r5/r3) quail to chick rhombomere transplants were performed at stage 10-12 (Fig. 2A), and operated hindbrains were assessed at stage 26-29 (Table 1A). Whole-mount in situ hybridisation on operated embryos showed that the transposed r5 maintained *Islet2* expression in the ectopic r3 position (Fig. 2B), which suggests that, from stage 10 onwards, motoneurone progenitors within r5 are committed to express SM markers. Conversely, when r3 was transposed to the r5 position (r3/r5) at stage 10-12, the transposed r3 failed to express *Islet2* (Fig. 2L, Table 1A), implying that r3 has maintained its rostrocaudal identity and failed to generate SM neurones. Thus, both r5/r3 and r3/r5 grafts after stage 10 showed rhombomere autonomy in gene expression patterns and SM neurone production.

To investigate the axon trajectory of the ectopic r5/r3 SM neurones, transverse sections of quail-chick chimeras were double-immunostained with various combinations of antibodies against neurofilament heavy chain (NF), Islet2 protein (Islet2), a quail-specific antigen (QCPN) or a quail axon-specific antigen (QN) (*n*=6; Fig. 2O-Q). In separate experiments, an antibody against Lim3 protein was used in combination with QCPN and QN antibodies (*n*=3; data not shown). In both sets of experiments, the ectopic r5 contained Islet2-positive and Lim3-positive quail neurones, which were closely associated with quail axons exiting the neuroepithelium ventrally (Fig. 2P,Q; data not shown). These axons formed an ectopic ventral exit point, which was absent on the unoperated side of the embryo because BM neurones in r3 form dorsal exit points only. The likely identities of these ventrally-projecting neurones are therefore SM abducens and accessory abducens neurones, which express Islet2 and Lim3, respectively. Axons from resident trigeminal motoneurones within r3 normally project dorsorostrally to exit the neuroepithelium in r2 (Fig. 1A). On the operated side at r2 level, quail axons extended via the trigeminal nerve dorsal exit point (data not shown), probably reflecting the pathways of facial motor axons from the transplanted r5, as has been shown previously in r5/3 grafts (Guthrie and Lumsden, 1991).

Do SM neurones within the r5 transplanted to r3 join the pathway of the endogenous abducens nerve? During normal development, abducens axons emerge from r5 and r6 as multiple rootlets, which fasciculate ventral to the brain, and extend rostrally to innervate the lateral rectus eye muscle, and the small pyramidalis and quadratus nictitans (P/Q) muscles (Wahl et al., 1994). In immunostained transverse sections of r5/r3 embryos, quail-derived axons exiting ventrally joined the host abducens nerve as it extended beneath the brain (Fig. 2Q),

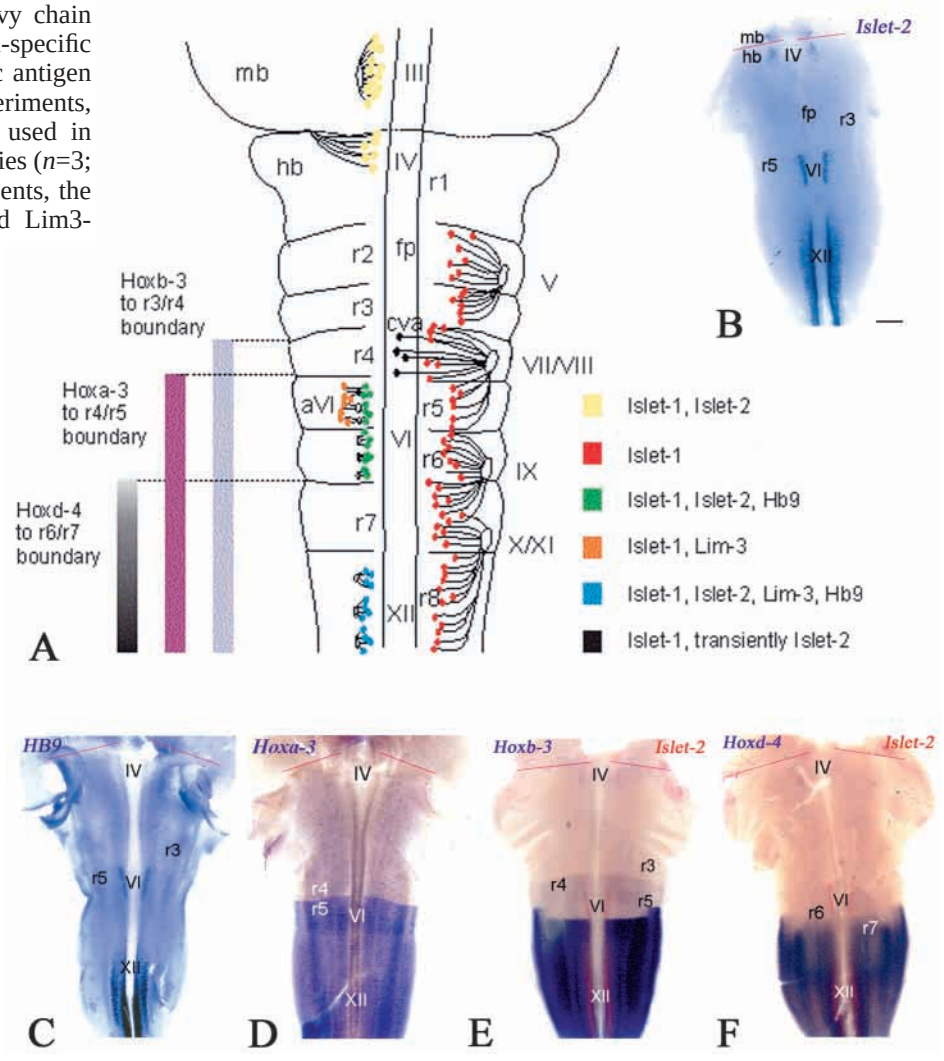

Fig. 1. Patterns of gene expression in rhombomeres and cranial motoneurones. (A) Diagram of a flat-mounted stage 28 chick embryo hindbrain and caudal half of the midbrain showing the different combinations of Lim homeobox genes expressed by each motor nucleus and the expression pattern of three Hox genes, *Hoxa3*, *Hoxb3* and *Hoxd4*. Rhombomere boundaries are no longer visible at this stage but are shown for clarity. Motor nuclei: III, oculomotor; IV, trochlear; V, trigeminal; VI, abducens; VII, facial; IX, glossopharyngeal; X, vagus; XI, accessory; XII, hypoglossal [adapted, with permission, from Varela-Echavarría et al. (Varela-Echavarría et al., 1996)]. (B-F) Flat mounts of E6 chick midbrain and hindbrain preparations. Red lines indicate the midbrain-hindbrain boundary. Whole-mount in situ hybridisation for *Islet2* (B), *Hb9* (C), *Hoxa3* (D), *Hoxb3/Islet2* (E) and *Hoxd4/Islet2* (F). mb, midbrain; hb, hindbrain; r, rhombomere; fp, floor plate; a, accessory; cva, contralateral vestibuloacoustic. Scale bar: 500 μm.

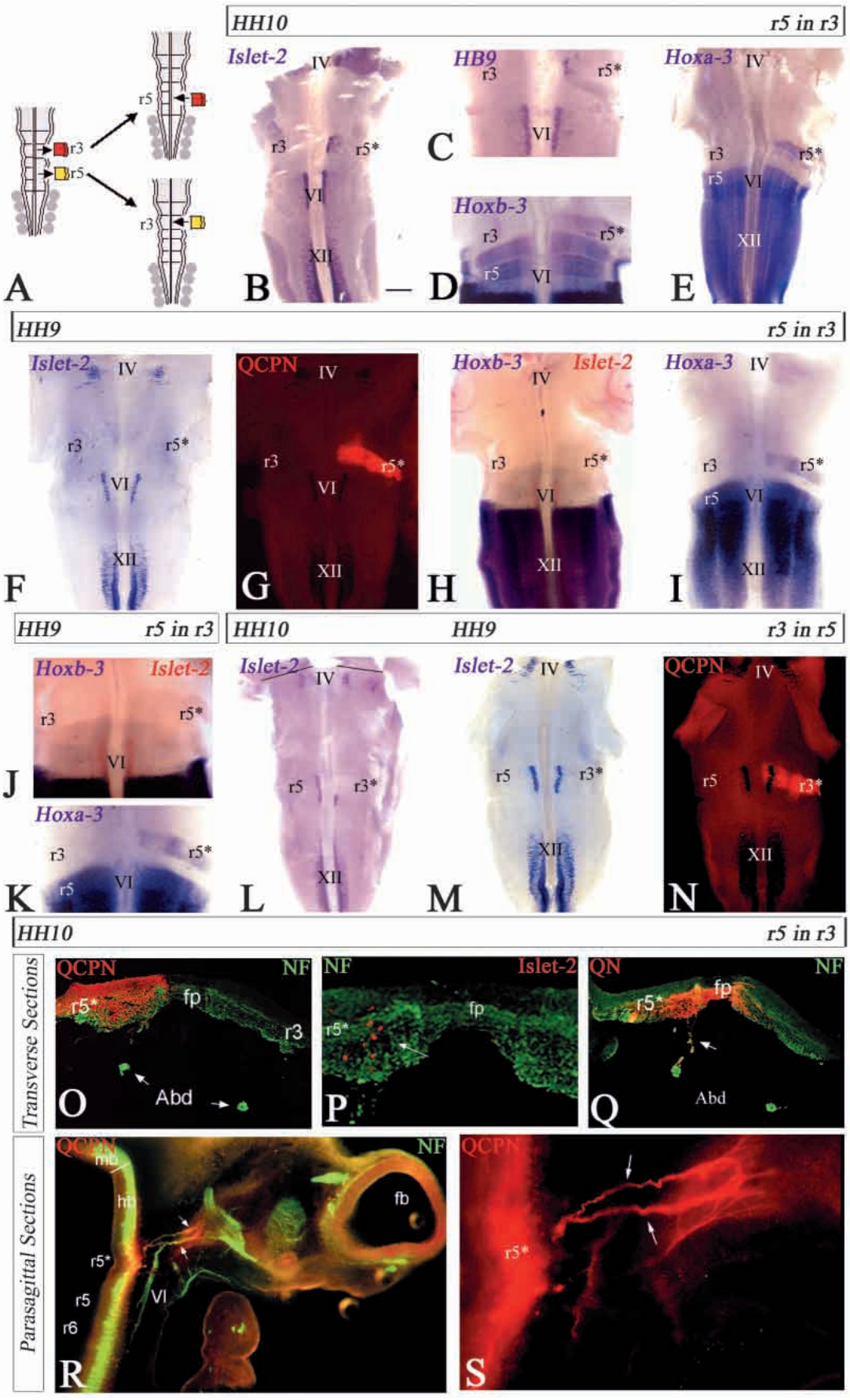

Fig. 2. Rhombomere grafts in the pre-otic region. (A) Transplant of r3 at level of r5 (r3/r5) and of r5 at level of r3 (r5/r3). (B-N) Flat mount of E6 chick/quail chimera hindbrains in situ hybridised with probes for *Islet2*, *Hb9*, *Hoxa3* or *Hoxb3* as indicated. Labels in white bars above each panel indicate the type of graft and embryonic stage at which the graft was undertaken. Asterisk indicates grafted rhombomere. (G,N) Additional immunostaining of the embryos in F and M, respectively, with anti-quail cell antibodies (QCPN) to show position of the graft. (J,K) Higher magnification of H and I, respectively. (O-S) Double-immunostaining (except S; single immunostaining) on sections of an E6 embryo that had received an r5 in r3 graft at stage 10; transverse cryostat sections through r3 (O-Q) or parasagittal vibratome sections (R,S). (S) Higher magnification of R. Antibodies as indicated: QCPN, anti-quail cells; NF, anti-neurofilament; QN, anti-quail axons; Islet2, anti-Islet2. r, rhombomere; HH indicates Hamburger/Hamilton staging of embryo. White arrows indicate: (O,Q-S) axonal bundles from the graft joining the host abducens (Abd); (P) r5* Islet2-positive motoneurones. Scale bar: 580 μm for B,E,F-I,L-N; 400 μm for C,D,J,K; 240 μm for O,Q; 120 μm for P; 500 μm for R; 350 μm for S.

Table 1. Summary of neural tube grafting studies

A Pre-otic

		Whole-mount in situ hybridisation for												
		Islet2			*Hb9*			*Hoxa3*			*Hoxb3*			
Stage	Graft	cs	os	*n*	cs	os	*n*	cs	os	*n*	cs	os	*n*	T
10/12	r5 in r3	+++	+++	9	+++	+++	3	+++	+++	3	+++	+++	4	19
9	r5 in r3	+++	–	11	nd			+++	+	3	+++	+	3	17
10/12	r3 in r5	–	–	3	nd			nd			nd			3
9	r3 in r5	–	+++	3										3
														42

B Post-otic

		Whole-mount in situ hybridisation for															
		Islet2			*Hb9*			*Hoxa3*			*Hoxb3*			*Hoxd4*			
Stage	Graft	cs	os	*n*	cs	os	*n*	cs	os	*n*	cs	os	*n*	cs	os	*n*	T
10/11	r3 in r8a	+++	–	3	+++	–	4	+++	+++	3	+++	+++	3	+++	+++	6	19
9	r3 in r8a	+++	+	2	nd												2
10/11	r3 in r8p	+++	–	6	+++	–	3	nd			nd			nd			9
9	r3 in r8p	+++	++	7	nd												7
10/11	r4 in r8a	+++	–	5	+++	–	3							+++	+++	3	11
11	r4 in r8p	+++	+	3	nd												3
10	r4 in r8p	+++	++	5	+++	++	2	nd			nd			nd			7
9	r4 in r8p	+++	+++	4	nd												4
																	62

n, number; T, total number; cs, control side; os, operated side; nd, not done.

whereas in parasagittal sections quail-derived axons fasciculated with the endogenous abducens and accessory abducens axons to extend towards the LR and P/Q muscles close to the orbit (Fig. 2R,S; *n*=4). It appears therefore that as early as stage 10, motoneurone progenitors in r5 are committed to express SM markers and to pursue an abducens pathway.

In pre-otic transplantations, rhombomeres show plasticity at stage 9

To pinpoint the stage at which rhombomeres become committed to generate SM neurones, transplantation experiments were performed at stage 9 (Table 1A). Following r5/r3 transplants at this stage, the transposed rhombomere failed to express *Islet2*, even though QCPN immunostaining showed that the graft was correctly located and integrated (Fig. 2F,G). Thus, SM neurones were not generated in the transplanted r5, which behaved according to the new location. Conversely, in r3/r5 transplants at stage 9, *Islet2* expression was induced, reflecting SM neurone production (Fig. 2M,N). Hence, in both caudal to rostral and rostral to caudal transpositions in the pre-otic region, cranial motoneurone rostrocaudal identity is susceptible to environmental cues at stage 9, but is fixed by stage 10.

Caudal to rostral rhombomere transpositions in the chick as early as stage 8+ have shown that the expression of Hox genes is maintained autonomously (Guthrie et al., 1992; Kuratani and Eichele, 1993; Simon et al., 1995), and it has been suggested that other aspects of rhombomere identity are also fixed (Grapin-Botton et al., 1995). However, our experiments show that, up to stage 9, *Islet2/Hb9* expression changes in pre-otic rhombomere transplants according to their new position. We therefore investigated the relationship between Hox genes and SM neurone formation using whole-mount single and double in situ hybridisation with *Islet2* and/or *Hoxa3/Hoxb3* probes on r5/r3 embryos (Table 1A). In r5 to r3 transplants performed at stage 9 and at stage 10, the transposed r5 maintained expression of *Hoxa3* and *Hoxb3* (Fig. 2D,E,H-K). Because in grafts at stage 9, the transplanted r5 did not express *Islet2* (Fig. 2F,G), there is a discrepancy between Hox gene expression and cranial motoneurone identity at this stage. However, *Hoxa3 and Hoxb3* expression in the transposed r5 was lower than in the host r5, at both stage 9 and stage 10.

In pre-otic to post-otic rhombomere transplants, SM neurone production can be induced

Previous studies have shown that rostral rhombomeres transposed caudally (to post-otic levels) show caudalised Hox gene expression profiles due to mesoderm-derived signals (Grapin-Botton et al., 1997; Grapin-Botton et al., 1995). To further investigate SM neurone production in relation to other aspects of rhombomere phenotype, we grafted r3 or r4 into the rostral or caudal part of r8 (r8a or r8p; level of somite 2 or 4, respectively) and analysed Hox gene expression (Fig. 3A; Table 1B). For grafts at stage 10-11, *Hoxa3*, *Hoxd4* and *Hoxb3* were all induced in the ectopic r3 in r8a or in r8p (Fig. 3B-D; data not shown), whereas *Islet2* and *Hb9* were not (Fig. 3E-G). Only at stage 9 did r3 express *Islet2*; the induced level of *Islet2* expression was higher in grafts in r8p than in grafts placed in r8a, but overall the expression level was lower than on the control side (Table 1B; data not shown). These data suggest that r3 is capable of responding to post-otic environmental signals by producing SM neurones, but only up to stage 9, reflecting a similar time dependence to its behaviour in r3 to r5 grafts.

Rhombomere 4 transplanted in r8a position at stage 10-12 failed to express SM markers (Fig. 3H; data not shown). However, r4 showed an increased tendency to generate SM neurones compared with r3 when transplanted to r8p position (Fig. 3I,J; data not shown), showing induction of SM neurones at stage 9, 10 and even 11, although the level of *Islet2* expression showed a progressive decrease at stage 10 and then

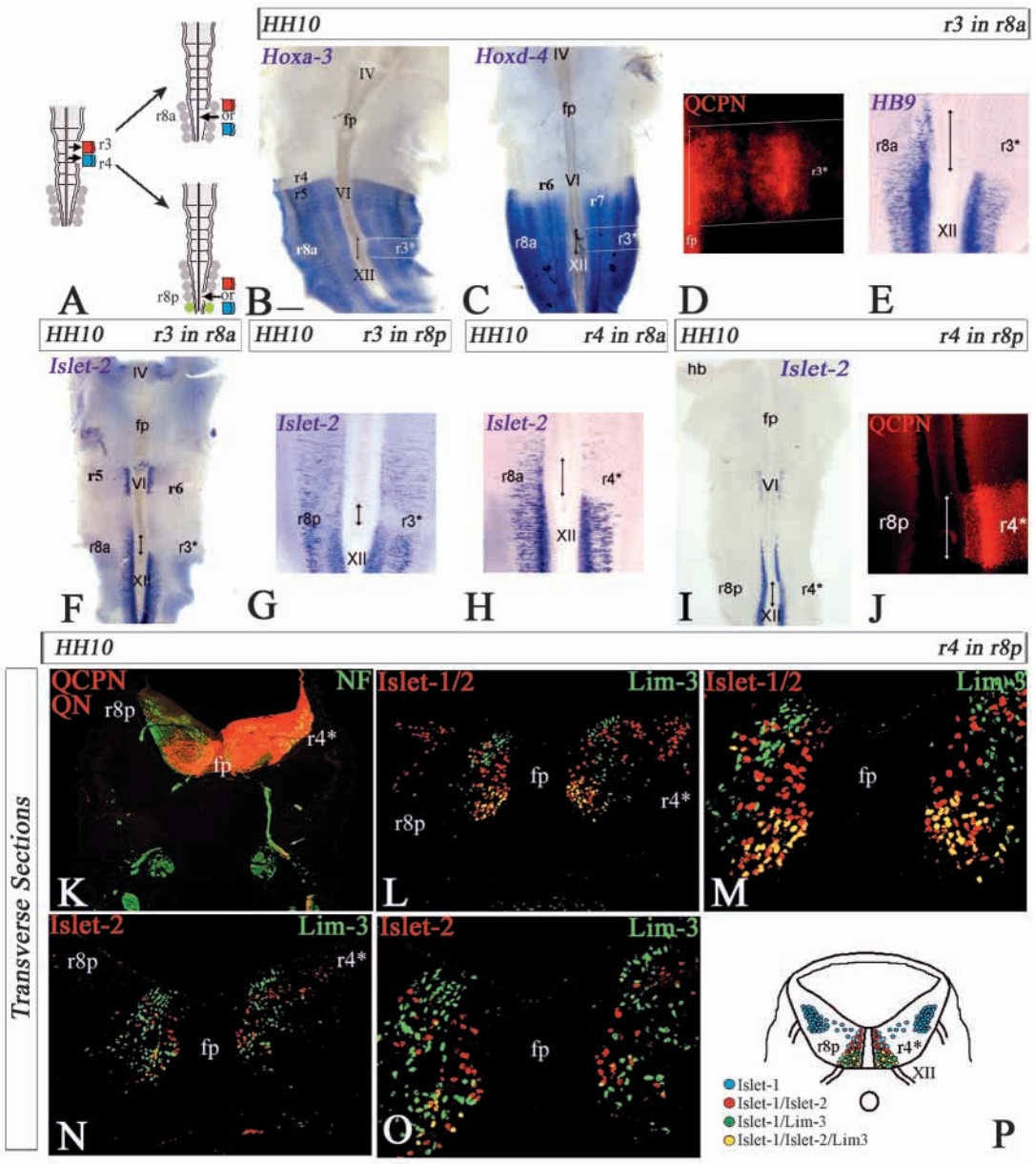

Fig. 3. Rhombomere grafts in the post-otic region. (A) Transplant of r3 or r4 at level of anterior (r8a) or posterior (r8p) r8. (B-J) Flat mounts of E6 chick/quail chimera hindbrain preparations containing rhombomere grafts, in situ hybridised with probes for *Islet2*, *Hb9*, *Hoxa3* or *Hoxd4* as indicated by blue type. Labels in white bars above each panel indicate the type of graft and embryonic stage at which the graft was undertaken. E,G and H show only the r8 region. Asterisk indicates grafted rhombomere. Double-headed arrows indicate rostrocaudal extent of grafted rhombomere. (D) Higher magnification of C showing immunofluorescent QCPN staining (red) of grafted r3. (J) Higher magnification of I showing immunofluorescent QCPN staining (red) of grafted r4. (K-O) Double-immunostaining on transverse serial cryostat sections (level of r8p) of E6 embryo that had received an r4 in r8p graft at stage 10. Antibodies as indicated as in Fig. 2, with the addition of anti-Islet1/2 and anti-Lim3 antibodies. White arrow (K) indicates quail axons from r4* leaving the neuroepithelium ventrally and joining host hypoglossal axons. (P) Diagram of a transverse section level of r8p summarising normal Lim code in host r8p versus grafted r4*. Scale bar: 580 μm for B,C,F,I; 190 μm for E,G,H,J; 140 μm for D; 340 μm for K; 120 μm for L,N; 60 μm for M,O.

stage 11 compared with stage 9 (Table 1B). These data highlight a contrast in the behaviour of r3 and r4, as in transplants at stage 10 into r8p, only r4, and not r3, was able to produce SM neurones. In addition, in such r3 grafts there was a lack of correspondence between Hox gene expression and SM neurone production, as caudal Hox genes were induced in the absence of a concomitant repatterning of SM neurones appropriate for that Hox 'code'.

In order to characterise further the putative SM neurones in r4 transplanted at stage 10, r4/r8p chimaeras were double-immunostained with various combinations of antibodies (n=7; Fig. 3K-O). Quail cells in the ectopic r4 expressed Islet2 protein, and quail axons exited ventrally from the neuroepithelium to fasciculate with chick hypoglossal axons (Fig. 3K,N,O). Some quail axons also exited the neuroepithelium dorsally, which suggests that some r4 motoneurones projected along vagus and cranial accessory axon pathways (data not shown). To confirm the hypoglossal identity of the newly induced SM neurones, the Lim homeobox 'code' of the transposed r4 was also investigated. Previous studies showed that r8 contains two distinct populations of motoneurones: vagus and cranial accessory neuronal somata are located laterally and express Islet1, whereas hypoglossal neurones lie more medially and express Islet1, Islet2 and Lim3 (Varela-Echavarría et al., 1996). We examined the Lim homeoprotein expression profiles of hypoglossal neurones in more detail at E6 in caudal r8, using antibodies against Islet1/2, Islet2 and Lim3 proteins. Because all motoneurones still express Islet1 at this developmental stage (Varela-Echavarría et al., 1996), we can conclude that hypoglossal neurones

express Islet1 and Islet2 or Lim3, with a subset co-expressing Islet2 and Lim3 (Fig. 3L-P). Each of these neuronal subpopulations occupied specific locations, with respect to the dorsoventral and mediolateral axes, that were distinct from those of abducens neurones at r5/6 level. For example, Islet2/Lim3-positive neurones were located medially and close to the ventral (pial) side of the neuroepithelium (Fig. 3O). Double-immunostaining on adjacent sections showed that the Lim homeobox code of the grafted r4/r8p mirrored perfectly that of the control r8 side (Fig. 3L-P), which shows that signals at r8p level could repattern r4 so that at least a proportion of motoneurones adopted a hypoglossal identity.

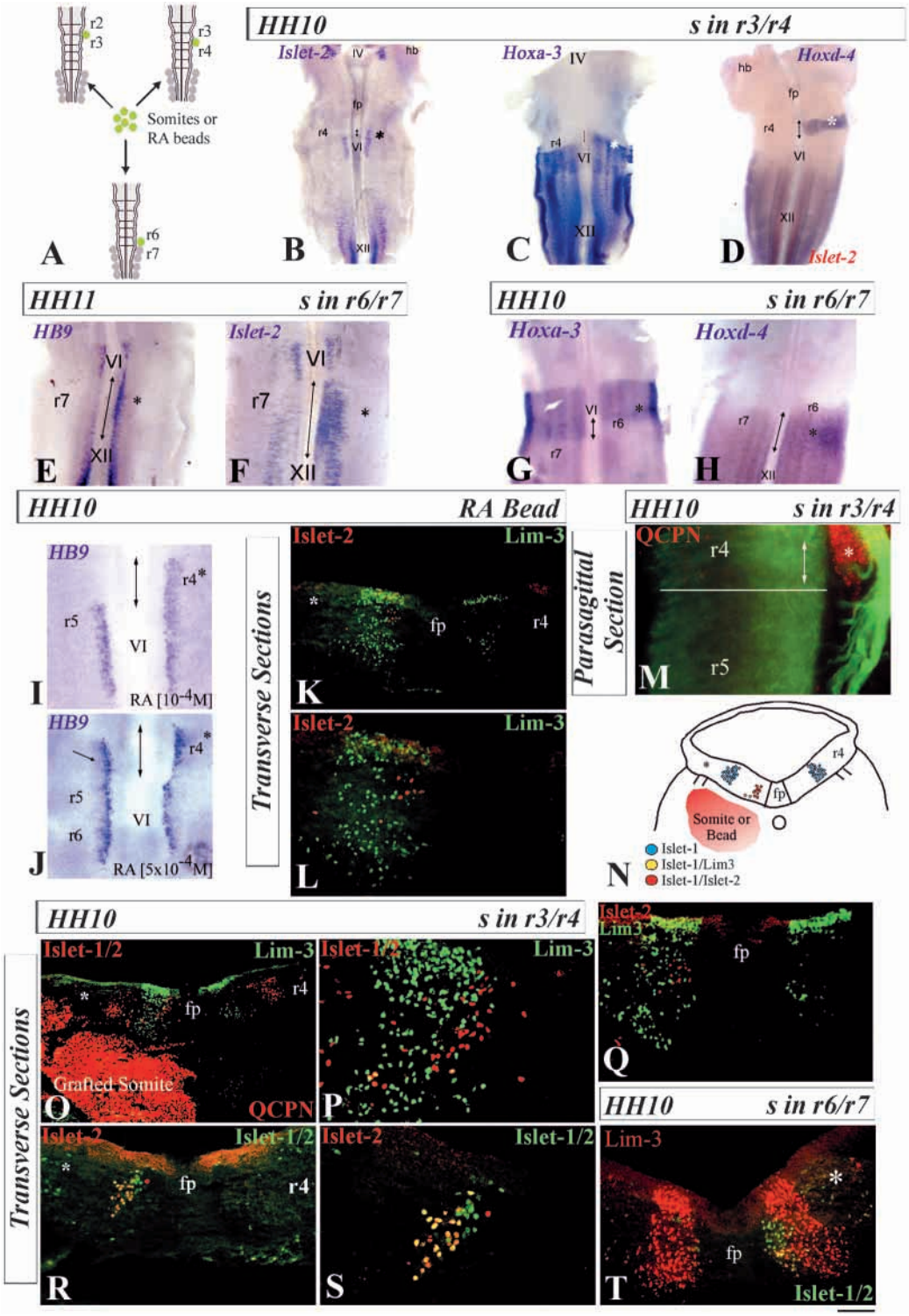

Fig. 4. Somite or RA-loaded bead grafts. (A) Somite and RA bead grafts at the level of r2/r3, r3/r4 and r6/r7. (B-J) Flat mounts of E6 chick hindbrain preparations after somite or RA bead grafts, in situ hybridised with probes for *Islet2*, *Hb9*, *Hoxa3* or *Hoxd4* as indicated. Labels in white bar above each panel indicate the type of graft and embryonic stage at which the graft was undertaken. (D) Double in situ hybridisation with probes for *Islet2* and *Hoxd4*. Asterisks indicate the grafted side and double-headed arrows indicate ectopic gene expression. (K-M,O-T) Double-immunostaining on a sagittal vibratome section (M) or transverse cryosections (K,L,O-T) of E6 chick embryos that have received a somite (M,O-T) or an RA bead graft (K,L) adjacent to the r3/r4 (O-S) or r6/r7 (T) level at stage 10. Antibodies are as indicated, abbreviations as in Figs 1-3. (M) Rhombomere boundaries are shown by a white line whereas the white asterisk highlights r4 ectopic SM axons. (O) QCPN stains the mesoderm, identifying the grafted somite (as in M). P and S are higher magnifications of O and R, respectively, showing the grafted side only. (N) Diagram of a transverse section of a chick embryo at the level of r4 summarising the normal Lim code on the control side (right) in comparison with the one on the somite/RA bead-grafted side (left). Although Islet1-positive motoneurones are present on either side, only the grafted side contains Islet2-positive/Lim3-negative motoneurones, consistent with an abducens identity for the r4 ectopic SM neurones. Note that when the somite was grafted at the level of r6/r7 the grafted side contains Islet2/Lim3-positive motoneurones consistent with a hypoglossal identity for the r7 ectopic SM neurones (see also Fig. 3P). Scale bar: 720 μm for B-D; 480 μm for E-H; 190 μm for I,J; 60 μm for L,P,S; 100 μm for M; 120 μm for K,Q,R,T.

SM neurones can be induced by signals from the paraxial mesoderm

Because somites transplanted into the pre-otic region could repattern Hox genes and neuronal differentiation (Grapin-Botton et al., 1997; Itasaki et al., 1996), we tested a possible influence of the caudal paraxial mesoderm on somatic motoneurones. Quail somites were grafted into isochronic chick hosts (stage 9-11) at various levels within the cranial paraxial mesoderm and beneath the neuroepithelium (Fig. 4A; Table 2A), and induction of *Islet2*, *Hb9*, *Hoxd4* and *Hoxa3* was analysed at E6. For grafts of rostral somites (s1 to s3) beneath the rostral hindbrain (r2-4) none of the markers assayed were induced, which indicates that these somites are devoid of inductive capability at the stages tested (9-12), which is consistent with previous data (Itasaki et al., 1996). When caudal somites (s5 or more caudal) were grafted underlying r2 and r3 at stage 9-11, no *Islet2* induction was observed, whereas *Hoxd4* induction was observed in the alar plate of r2 and r3 (Table 2A; data not shown). Grafting of caudal somites underlying r3 and r4 at stage 11 led to a similar failure of SM neurone differentiation, and induction of *Hoxd4* in the r3 and r4 alar plate only (Table 2A; data not shown). However, for transplants at stage 9-10, both *Islet2* and *Hb9* were induced in r4, although in some cases this was limited to the caudal region (Fig. 4B; data not shown). In these grafts, *Hoxa3* and *Hoxd4* expression was, in some cases, induced in the alar plate of r3 (data not shown) but was induced in r4 extending ventrally as far as the floor plate, corresponding with the region of SM neurone induction (Fig. 4C,D).

The phenotypes of the ectopic r4 SM neurones in somite-grafted embryos were analysed as described previously. In all cases (n=4), ectopic axons at r4 level exited the neuroepithelium ventrally as small rootlets and fasciculated with the endogenous abducens axons to extend towards the eye (Fig. 4M). To confirm an abducens phenotype of these neurones, transverse sections were double-immunostained to ascertain the Lim homeoprotein profile (Fig. 4O-S). As summarised diagrammatically (Fig. 4N), both the control and the somite-grafted side contained a lateral Islet1-positive motoneurone population belonging to the facial nucleus (blue), which was immunostained with pan-Islet1/2 antibodies but not anti Islet2 antibodies (Fig. 4N,O,R; data not shown). Only the somite-grafted side contained a medial Islet1/Islet2 positive, Lim3 negative motoneurone population (red), and a smaller Islet1/Lim3 positive population (yellow; Fig. 4N,P-S). On the basis of their Lim code, these two populations are likely to represent the abducens and accessory abducens neurones, respectively, with the abducens neurones positioned close to the ventricular side of the neuroepithelium and the accessory abducens neurones (Fig. 4N,P) positioned more laterally (Varela-Echavarría et al., 1996). No Islet2/Lim3-positive neurones were detected, which would have represented a hypoglossal phenotype (Fig. 4N,Q). Hence, at stage 9-10, somite-derived caudalising signals acting at the level of r4 repatterned r4 to produce SM neurones with abducens identity.

The apparent abducens identity of ectopic SM neurones following somite transplants presents a paradox, because the expression of *Hoxa3* and *Hoxd4* together (in embryos analysed 76 hours post-grafting; Table 2A) is consistent with a hypoglossal rather than an abducens phenotype. A possible reconciliation of these data lies in previous studies showing that following rostral somite transplants, caudal Hox genes take longer to be induced in rostral rhombomeres than more rostral Hox genes (Grapin-Botton et al., 1997; Itasaki et al., 1996). We therefore analysed Hox gene expression 24, 36 and 48 hours after somite grafting. After 24 hours, neither *Hoxa3* nor *Hoxd4* were expressed, whereas after 36 hours *Hoxa3* but not *Hoxd4* was expressed, and after 48 hours both *Hoxa3* and *Hoxd4* were expressed (Table 2B). These data demonstrate that there is indeed a timelag in *Hoxd4* induction in response to somite-derived signals, so that although *Hoxa-3* is switched on at the equivalent of stage 15/16, *Hoxd4* expression is not initiated until approximately stage 20. This may be consistent with the acquisition of an abducens phenotype by ectopic SM neurones in r4.

In order to further test the effects of somite grafts, we took

Table 2. Summary of somite grafting studies

A

		Whole-mount in situ hybridisation for								
		Islet2		*Hb9*		*Hoxa3*		*Hoxd4*		
Stage	Graft	Induction	*n*	Induction	*n*	Induction	*n*	Induction	*n*	T
9/10	s5 in r2r3	none	11	nd		nd		r2ap/r3ap	2	13
11	s5 in r3r4	none	7	none	2	nd		r3ap/r4ap	5	14
9/10	s5 in r3r4	r4	13	r4	5	r3ap/r4	4	r3ap/r4	2	24
11	s5 in r6r7	r7	3	r7	2	nd		nd r6/r7		5
10	s5 in r6r7	r7	4	r7	3		3		5	15
9/10	s1 in r3r4	none	5	nd		Repressed in r6 nd		nd		5
										76

s5, somite 5 caudally; s1, somite 1 to 3 only; *n*, number; T, total number; nd, not done; ap, alar plate.
NB in this table only gene expression in the grafted side has been presented.

B Time course

		Whole mount in situ hybridisation for						
		Hoxa3			*Hoxd4*			
Stage	Graft	24 hours	36 hours	48 hours	24 hours	36 hours	48 hours	T
9/10	s5 in r3r4	0/5*	4/4*	3/3*	0/3*	0/5*	3/3*	23
								23

*****Number of embryos ectopically expressing the marker/number of embryos analysed.

advantage of the fact that r7 does not express SM neurone markers (Fig. 1B,C). When caudal somites were grafted beneath r6/7 at stage 10-11 (Table 2A), *Islet2* and *Hb9* were induced in r7 at levels comparable to the rostral r8 expression, even at stage 11 (Fig. 4E,F). Thus, r7 was capable of responding to somite signals by generating SM neurones up until later stages of development than more rostral rhombomeres. We also tested the effects of somite transplants at r6/r7 level on *Hoxa3* and *Hoxd4* expression. When embryos incubated until E6 were subjected to in situ hybridisation for these genes but using shorter development times than usual, gradations in Hox gene expression between axial levels was apparent. For example, on the control sides of embryos (left hand side; Fig. 4G,H) *Hoxa3* was expressed at a higher level in r6 than it was caudally, whereas for *Hoxd4* the converse was true (see also Fig. 1D,F). However, for the operated, somite-grafted side, *Hoxa3* and *Hoxd4* expression were down- and upregulated, respectively, within the r6/7 region, reflecting a caudalisation of these rhombomeres (right hand side; Fig. 4G,H). Such a caudalisation was accompanied by the generation of Lim3/Islet1/2 neurones at medial positions, consistent with a hypoglossal identity adjacent to the transplanted somite (Fig. 4T; compare with Fig. 3M,P). In order to further confirm this hypoglossal identity, we sought to follow the axon pathway of induced SM neurones in r6/7, but were unable to trace nerve rootlets further than a short distance from the hindbrain (data not shown). However, the balance of evidence favours the idea that hypoglossal SM neurones were generated in r6/7 in response to somite grafts.

Taken together, these somite-grafting experiments indicate that there are rostrocaudal differences in the time-window during which cranial motoneurone progenitors are capable of responding to patterning signals from the somites. Rhombomere 7 is still capable of responding to these signals as late as stage 11, whereas r4 is refractory to these signals by stage 11, and r2 and r3 are not sensitive to the signal even as early as stage 9. These observations could imply either a complete inability of the rostral hindbrain to respond to somitic signals, or an earlier fate commission of rostral rhombomeres relative to more caudal levels. Finally, it is also possible that r2 and r3 require a higher level of inductive signal than a single grafted somite can supply.

Retinoic acid beads mimic the caudalising action of the somites

It has been proposed that retinoic acid (RA) mediates a part of the ability of the paraxial mesoderm to caudalise the rostrocaudal axis (Gavalas and Krumlauf, 2000; Gould et al., 1998). In the early chick embryo, the somitic mesoderm generates RA, with younger, more caudal somites generating higher levels of RA than older ones (Berggren et al., 1999; Maden et al., 1998; Swindell et al., 1999). As our somite grafting experiments showed that only caudal somites could induce SM neurones, this implies that RA is a candidate in SM neurone induction.

When beads treated with RA [10^{-4} M] were grafted in chick hosts at various axial levels within the cranial paraxial mesoderm and beneath the neuroepithelium (Fig. 4A; Table 3), *Islet2* and *Hb9* were induced exclusively in r4, and only in grafts at stage 9-10 at r3/4 level (Fig. 4I; Table 3). No induction was observed in grafts done at stage 11 or when beads were implanted at more rostral positions (data not shown; Table 3). When a higher concentration of RA was used (5×10^{-4} M), SM neurone induction was still exclusive to r4, although some *Hb9* induction was observed in the r4 contralateral to the bead implantation (Fig. 4J). We also analysed Hox gene expression following RA bead implantation. No induction of *Hoxa3* or *Hoxd4* was observed in transplants performed at stage 11. However, for transplants of beads treated with RA [10^{-4} M] at stage 9/10, five out of five cases showed *Hoxa3* induction, whereas three out of seven cases showed *Hoxd4* expression (Table 3). This lower frequency of *Hoxd4* expression was observed even when 5×10^{-4} M RA was used to soak the beads, in which case one out of three embryos showed induction (Table 3). The Lim homeobox gene expression of the ectopic r4 SM neurones was assessed in E6 embryos grafted at stage 10 (RA 10^{-4} M, n=3; RA 5×10^{-4} M, n=2), and Islet2 positive/Lim3 negative motoneurones were found on the grafted side (Fig. 4K,L). Hence, ectopic RA-induced SM neurones have an abducens phenotype, as in somite grafting experiments. The invariant induction of *Hoxa3* and lower frequency of induction of *Hoxd4* are broadly consistent with the abducens phenotype of the induced neurones.

The parallels between the results from somite grafting and RA bead grafting studies (compare Tables 2 and 3) support the idea that retinoic acid mediates a part of the caudalising ability of the paraxial mesoderm. Rhombomeres rostral to r4 did not respond to high concentrations of RA, even as early as stage 9, suggesting that the reason for the insensitivity of these rhombomeres to somite grafts in unlikely to be caused by an insufficiency of signal. Instead, such insensitivity might be explained by a suppressive effect of adjacent tissues, consistent

Table 3. Summary of RA bead grafting studies

		Whole-mount in situ hybridisation for								
		Islet2		*Hb9*		*Hoxa3*		*Hoxd4*		
Stage	Graft	Induction	*n*	Induction	*n*	Induction	*n*	Induction	*n*	T
9/10	RA^1 in r2r3	none	5	none	2	nd		nd		7
11	RA^1 in r3r4	none	4	none	3	none	3	none	8	18
9/10	RA^1 in r3r4	r4	2	r4	8	r4	5	r4	3/7†	17
10	RA^5 in r3r4	nd		r4*	5	nd		r4	1/3†	8
										50

*Some induction was observed also in the contralateral r4.
†Number of embryos ectopically expressing *Hoxd4* in r4/number of embryos analysed.
RA^1, 1×10^{-4} M; RA^5, 5×10^{-4} M.

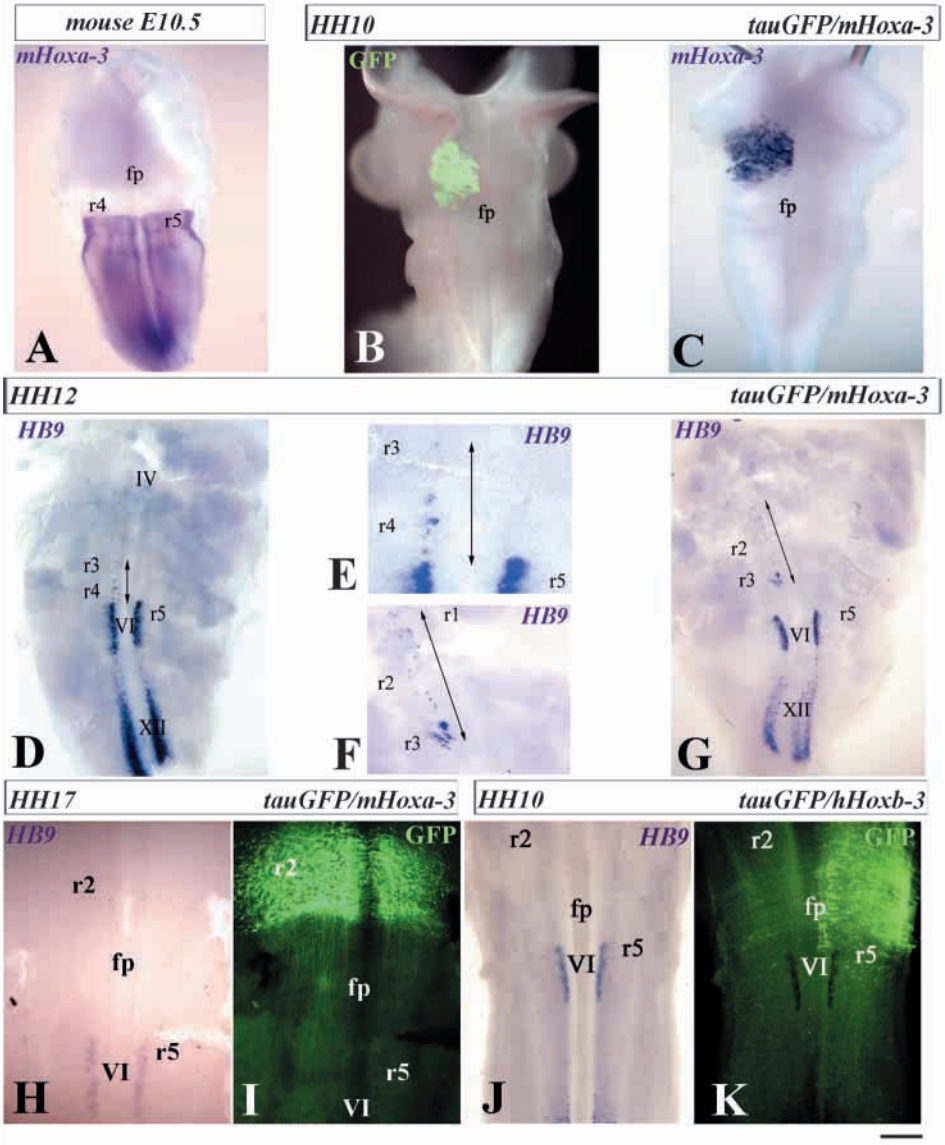

Fig. 5. Misexpression of *Hoxa3* in the rostral hindbrain. (A) Flat mount of mouse hindbrain (E10.5) in situ hybridised for mouse *Hoxa3*. (B,C) Dorsal view of a chick head electroporated on the left side with *tauGFP/Hoxa3* at stage 10 and incubated until E4, showing co-localisation of GFP fluorescence (B) and in situ hybridisation for *Hoxa3* (C). (D-I) Flat mounts of E4 chick hindbrains electroporated at stage 12 (D-G) or 17 (H,I) with *Hoxa3/tauGFP*, and in situ hybridised for *Hb9*. Double-headed arrow indicates *Hb9* induction. E and F are higher magnifications of D and G, respectively. (I) Same embryo as H following immunostaining for GFP protein to show the area of electroporation. Note that at stage 17 no *Hb9* induction was observed following electroporation of *tauGFP/Hoxa3*. (J,K) Flat mounts of the same E6 chick hindbrain electroporated with human *HOXB3/tauGFP* at stage 11, in situ hybridised for *Hb9* (J) and immunostained for GFP (K). Note that no induction of *Hb9* was observed. Scale bar: 580 μm for A-C; 420 μm for D,G; 250 μm for E,F; 300 μm for H,I; 500 μm for J,K.

with the observation that r3 can acquire a caudal identity when transplanted caudally, away from the influence of such signals.

Misexpression of *Hoxa3* is sufficient to induce ectopic SM neurones in the rostral hindbrain

Although most of our data indicate a correlation between rostrocaudal motoneurone identity and Hox gene expression, there were examples to the contrary. For example, in rostral to caudal grafts (r3/r8a), r3 expressed Hox genes typical of r8 identity, but failed to produce SM neurones. In order to test directly the role of Hox genes in specifying rostrocaudal identity of motoneurones, in ovo electroporation was used to misexpress the full-length *Hoxa3* cDNA in the rostral hindbrain of stage 8-16 embryos (r1-r4 region). *Hoxa3* is expressed from the rhombomere 4/5 boundary caudally (Fig. 1A,D) and is therefore a good candidate to impose an abducens phenotype on r5 and r6 motoneurones (Capecchi, 1997). To allow identification of the ectopic region of *Hoxa3* expression in the chick hindbrain, a mouse *Hoxa3* cDNA was used (Fig. 5A,C), and to facilitate the screening of electroporated embryos, a *tauGFP* plasmid was co-electroporated (Fig. 5B,C). The results of electroporation of the two constructs were compared with control electroporations of the *tauGFP* plasmid alone. GFP expression was observed in embryos 3 hours after electroporation, as previously reported (Momose et al., 1999). After 48 hours (equivalent of E4), embryos showing unilateral GFP expression in the rostral hindbrain were processed by whole-mount in situ hybridisation for *Hb9*. Ectopic *Hb9* motoneurones were found only in those embryos that had received both *tauGFP* and *Hoxa3* plasmids (n=21; Fig. 5D-G), but never in the control group (n=5; data not shown). Interestingly, each of rhombomeres 1 to 4 was found to produce *Hb9*-positive motoneurones in some cases, in contrast to the inability of r1-3 to generate SM neurones in somite or RA bead grafting experiments. In all embryos examined (n=5), some GFP-positive axons left the neuroepithelium from ectopic ventral exit points in the *GFP/Hoxa3* positive region, consistent with the induction of SM neurones (data not shown). To assess Lim gene expression patterns of these ectopic SM neurones, embryos were grown up to E5, and GFP fluorescence

was combined with double-immunostaining for anti-neurofilament antibodies and anti-Lim antibodies on serial sections (Fig. 6A-D). These experiments showed that a similar number of motoneurones were present in both the control and electroporated sides (Fig. 6A,B), but ectopic Islet2-positive motoneurones were present only on the GFP-positive electroporated side (Fig. 6A,C,D). The majority of Islet2-positive motoneurones were Lim3 negative, Which is indicative of an abducens phenotype, but occasional Islet2/Lim3-positive neurones were detected (Fig. 6C,D). Because in these experiments, embryos were fixed earlier (E5) than in other experiments (E6), this may reflect the fact that accessory abducens neurones (destined to be Islet1/Lim3) are in the process of migrating laterally and have yet to downregulate Islet2. Hence, misexpression of *Hoxa3* at stage 8-16 is sufficient to induce SM neurones in the rostral hindbrain. However, the number of motoneurones within the *Hoxa3* misexpression domain was relatively small compared with those at axial levels that normally generate SM neurones. Electroporation of *Hoxa3* at stage 17 or later failed to induce *Hb9* expression (Fig. 5H,I), showing that the window of competence to generate SM neurones extended only up to stage 16. As the domain of expression of *Hoxb3* also coincides with the region that generates SM neurones, we also tested whether misexpression of *Hoxb3* in r1-4 could induce ectopic SM neurones. However, co-electroporation of a human *HOXB3*

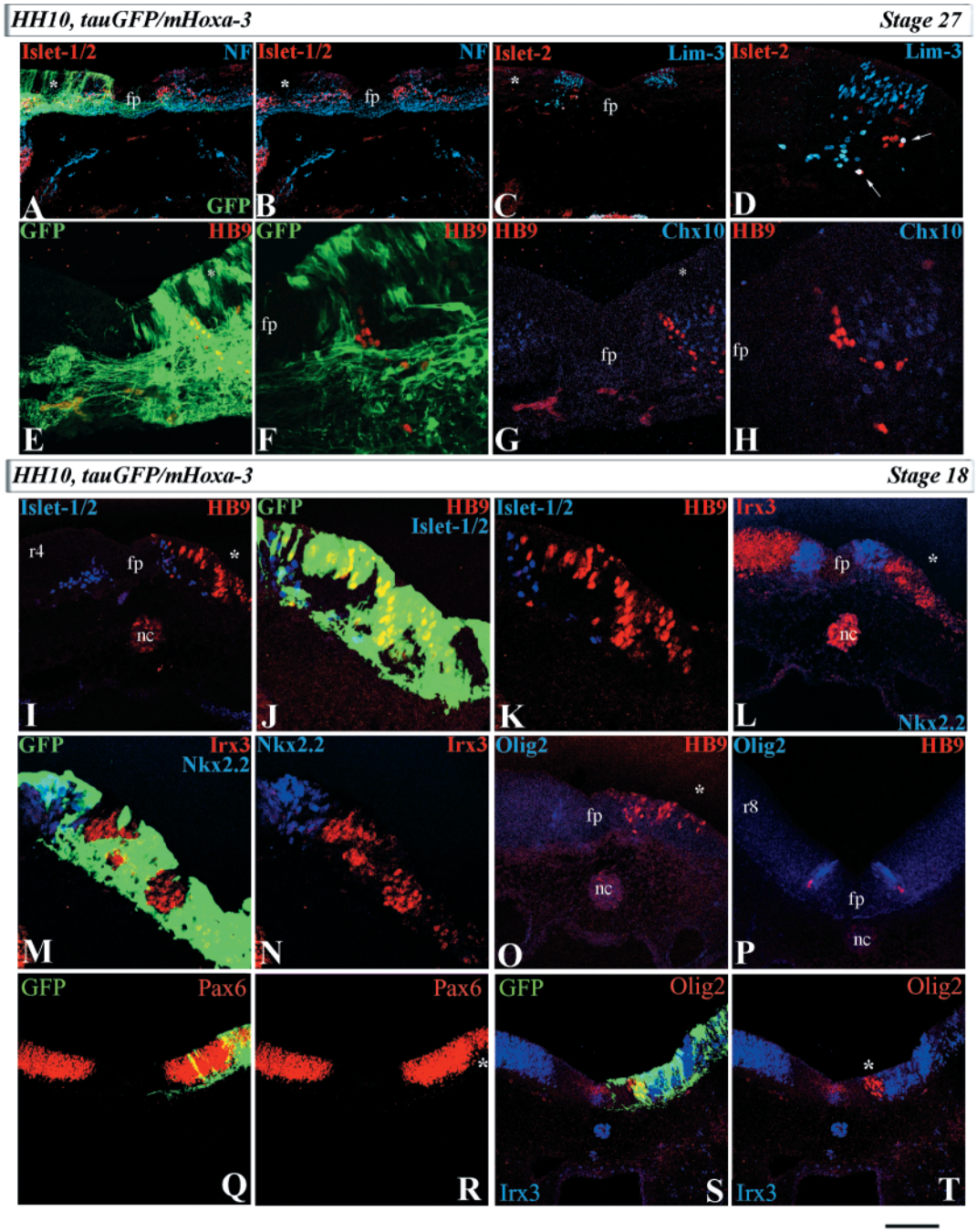

Fig. 6. Dorsoventral patterning following *Hoxa3* misexpression.
(A-T) Immunostaining on transverse cryostat sections of embryos electroporated with mouse *Hoxa3/tauGFP* at stage 10.
(A-D,E-H) Sections of two different embryos grown up to stage 27 prior to fixing.
(I-P) Sections through another embryo that was fixed at stage 18.
(Q-T) Sections through a second embryo fixed at stage 18. D,F,H,J-K,M-N are higher magnifications of C,E,G,I,L, respectively, showing only the electroporated side.
Antibodies are as indicated.
(A,E-F,J,M,Q,S) GFP natural fluorescence.
K,N,R,T are the same sections as J,M,Q,S, respectively, but without the GFP signal. White asterisks (A,B,C,G,I,L,O) indicate the electroporated side.
White arrows (D) indicate Islet2/Lim3-positive motoneurones. Asterisks (O,T) represent regions of repression of Pax6 and of induction of Olig2 expression, respectively.
(P) r8, (S,T) r1; all other axial levels shown are r3/4.
Scale bar: 120 μm for A,C,Q,T; 60 μm for D,E,G,I,L,O-P; 30 μm for F,H,J-K,M-N.

plasmid and a *tauGFP* plasmid at the same stages as for *Hoxa3* (stage 8-16) resulted in a few ectopic *Hb9*-positive cells in the rostral hindbrain in only two out of seventeen cases (data not shown), and in the majority of cases no SM neurone induction was observed (Fig. 5J,K). Thus the effect of *Hoxb3* in SM neurone induction appears to be weak or absent compared with that of *Hoxa3*.

Dorsoventral patterning is altered following *Hoxa-3* misexpression in the rostral hindbrain

The induction of SM neurones in the rostral hindbrain by *Hoxa3* electroporation suggests that dorsoventral patterning has been altered in this region. In the hindbrain, BM/VM neurones originate from a domain of the neural tube that lies directly adjacent to the floor plate, the p3 domain, which is *Nkx2.2*-positive (Briscoe et al., 1999). In the spinal cord and caudal hindbrain, SM neurones originate from a domain dorsal to this, the pMN domain, which is *Olig2*-positive, *Nkx2.2*-negative and which expresses *Pax6* at low levels (Briscoe et al., 1999; Novitch et al., 2001; Ericson et al., 1997). Lying dorsal to the pMN domain is the p2 domain, which is *Olig2* and *Nkx2.2*-negative, and which expresses *Pax6* at high levels and in addition expresses *Irx3* (Briscoe et al., 2000). The p2 domain gives rise to interneurones that express the marker *Chx10*. However, the disposition of these domains within the rostral hindbrain has not been extensively investigated as it has been in the spinal cord. We found that in rhombomeres 2-4 of the rostral hindbrain at stage 18, the domains of *Nkx2.2* (p3) and *Irx3* (p2) expression abutted each other directly, without an intervening pMN domain (Fig. 6L) (C. William and T. Jessell, personal communication; J. Ericson, personal communication). It might also be expected that a domain of high Pax6 expression (p2) would directly abut the Nkx2.2 domain (p3) in the rostral hindbrain, rather than include an intervening domain of low Pax6 expression (pMN) as has been reported (e.g. Ericson et al., 1997). However, we were unable to detect any gradations in Pax6 expression in the hindbrain, at least at its ventral limit (Fig. 6R). However, this may have reflected a technical limitation in the sensitivity of our immunohistochemistry.

In *Hoxa3* electroporated embryos, we performed double immunostaining on transverse sections showing GFP expression, to visualise the domains of expression of various dorsoventral markers of progenitor domains or cell fate. In particular, we focused on patterning changes in regions in which ectopic SM neurones were present, as shown by immunopositivity using an antibody against the SM markers Mnr2/Hb9 (and which we shall refer to as Hb9-positive cells). In embryos analysed at stage 27, Hb9-positive induced SM neurones were located ventrally within the hindbrain, and were in some cases interspersed with or ventral to Chx10-positive interneurones (Fig. 6E-H). As the location of these cells would be consistent with the conversion of the p2 domain into an ectopic pMN domain, we analysed whether at earlier stages (e.g. stage 18) Olig2 had been induced in the GFP/Hb9-expressing domain. At this stage, ectopic Hb9-postitive cells were observed laterally as well as ventrally, which suggests that some more laterally-located cells may die, leading to the ventral localisation of Hb9-postitive cells observed at stage 27 (Fig. 6I-K). Only a few of the most ventral of these Hb9-positive cells were Islet1/2-positive, which is consistent with this idea (Fig. 6K; data not shown). However, no ectopic Olig2 was detected at r2-4 levels (Fig. 6O), despite the presence in the same embryo of an Olig2-postitive domain at rhombomere levels 5-8 where resident Hb9-positive motoneurones were also detected (Fig. 6P). However, Olig2 expression was induced coincident with ectopic Hb9-postitive cells in caudal r1 in response to *Hoxa3* overexpression (Fig. 6S,T), perhaps reflecting an enhanced tendency for r1 to produce SM neurones (the SM trochlear nucleus lies in rostral r1 although it is Hb9-negative; see Fig. 1).

The p2 marker Irx3 was repressed in GFP-expressing regions within r2-4 (Fig. 6L-N,S,T). *Irx3* and *Olig2* have been shown to be mutually repressive (Novitch et al., 2001), and yet these data suggest that *Hoxa3* is capable of repressing *Irx3* and inducing SM neurones without induction of *Olig2*. The localisation and level of Nkx2.2 expression failed to change following *Hoxa3* overexpression (Fig. 6L), whereas Pax6 expression was repressed to a modest extent, and particularly in dorsal regions (Fig. 6Q,R). Taken together, the downregulation of both Irx3 and Pax6 would be consistent with the induction of an ectopic pMN domain that generates ectopic SM neurones, although this domain apparently lacks Olig2 expression.

DISCUSSION

Our first major conclusion is that the capacity of a rhombomere to produce SM neurones is susceptible to alteration by rostrocaudal cues, but becomes fixed at stage 10-11 at around the stage of neural tube closure. Second, grafting of somites or RA beads in the rostral hindbrain induces SM neurones, which suggests that RA might be a component of somite-derived signals that pattern SM neurones in vivo. Third, SM neurone induction by somite grafts or by RA is concomitant with ectopic Hox gene expression, such as *Hoxa3*. Fourth, misexpression of *Hoxa3* in the rostral hindbrain alters dorsoventral patterning and induces ectopic SM neurones, which implies that Hox genes expressed in r5-8 might be involved in patterning SM neurones.

Cranial motoneurone identity is plastic prior to neural tube closure

Our data indicate that cranial motoneurone commitment to a particular rostrocaudal identity must occur in a very restricted time period at stage 10-11 and coincident with the time of neural tube closure. These results are broadly comparable to those for the spinal cord, in which motoneurone progenitor identity is labile at stage 11 but becomes fixed just a few hours later, at around stage 12 (Ensini et al., 1998; Lance-Jones and Landmesser, 1980; Matise and Lance-Jones, 1996). In the hindbrain the first post-mitotic motoneurones are detected using Sc1 and Islet1 markers at late stage 13 (Ericson et al., 1992; Guthrie and Lumsden, 1992; Varela-Echavarría et al., 1996). As the acquisition of a generic motoneurone fate remains sensitive to local Shh signalling until late in the final cell cycle of motoneurone progenitors (Ericson et al., 1996), rhombomere commitment to generate a particular repertoire of motoneurones occurs relatively early in the process of motoneurone fate specification.

Rostrocaudal patterning of cranial motoneurones by the paraxial mesoderm and RA

Our results from transplantation experiments are consistent with the existence of a mesoderm-derived caudalising activity that is capable of eliciting somatic motoneurone differentiation from at least a subset of progenitors. The timing and modality of action of such a caudalising activity differs along the rostrocaudal axis, with caudal rhombomeres being more susceptible than rostral ones. Prior to stage 10, both r3 and r4 were competent to express *Hb9/Islet2* and produce SM neurones in response to somite signals when transplanted into r8 caudal position. However, by stage 10 only r4, and not r3, could generate SM neurones following transposition to r8, whereas at stage 11, r7 was still capable of responding to caudal signals. This suggests that the competence to respond to somite signals by SM neurone differentiation decreases with time, and is switched off more rapidly in r3 than in r4 and more caudally. Moreover, there appears to be a gradient of signals along the rostrocaudal axis, because for the same rhombomere (r4) transplanted at the same stage (10/11), *Islet2* was induced in grafts made into the caudal but not the rostral part of rhombomere 8.

In caudal rhombomere transpositions, caudalising signals are likely to come from the somites, an idea supported by the results of somite grafting experiments. Somites transplanted beneath the neural tube at r2-4 levels induced SM neurone differentiation in r4, as well as a caudalisation of Hox gene expression. Perhaps surprisingly, somite grafts did not induce SM neurones in r3, even at a stage (stage 9) at which transplantation of r3 tissue to caudal r8 (adjacent to s5) would have resulted in SM neurone differentiation. This may suggest the existence of factors capable of repressing the caudalising agent, localised in rostral rhombomeres and/or the rostral (pre-otic) paraxial mesoderm. We found that r4 also manifested a differential response to caudal transplantation or juxtaposition of a somite, as in the former case hypoglossal neurones were induced, whereas in the latter case abducens neurones formed. The explanation for this finding appeared to be that *Hoxa3* expression was induced in r4 more rapidly than *Hoxd4*, which is consistent with previous studies (Grapin-Botton et al., 1997; Itasaki et al., 1996). Expression of *Hoxa3* in the absence of *Hoxd4* is consistent with an abducens motoneurone phenotype, and by the time *Hoxd4* was switched on, motoneurone fates and axon pathways might already have been established.

We have found that the rostral implantation of RA beads mimicked the action of the somite, inducing SM neurones in r4, but not r3, and with an identical stage dependence. Indeed, it has been proposed that RA mediates a part of the caudalising ability of the paraxial mesoderm in patterning the rostrocaudal axis (Berggren et al., 1999; Gavalas and Krumlauf, 2000; Gould et al., 1998; Maden et al., 1998; Swindell et al., 1999), and RA is produced by the somites (Maden et al., 1998). Our finding that only somites caudal to s5 were capable of inducing SM neurones is also consistent with the idea that RA is involved, because RA is generated at a high level in younger somites (Maden et al., 1998; Swindell et al., 1999) and the ability of the somites to repattern Hox gene expression is lost in a rostral to caudal wave (Itasaki et al., 1996). It is thus possible that RA influences SM neurone patterning through a rostral (low) to caudal (high) gradient in the somitic mesoderm and possibly the hindbrain (for a review, see Maden, 1999). Application of RA beads reliably induced *Hoxa3* but only induced *Hoxd4* in a proportion of cases, in contrast to the invariant induction of *Hoxd4* in somite grafts. This observation may be consistent with studies showing that somitic signals capable of inducing *Hoxd4* are not entirely accounted for by RA; a higher molecular weight factor is involved (Gould et al., 1998). In view of the lack of RA-mediated induction of SM neurones in r3, higher doses of RA were applied: this did not induce ectopic SM neurones in r3, but instead induced SM neurones on both sides of r4. These results also tend to favour the idea that r3 or its surrounding mesoderm contains an inhibitory factor that modulates the action of RA, preventing SM neurone differentiation. Indeed, our recent results from in vitro experiments have shown that the ability of RA to induce SM neurones in the rostral hindbrain is modulated by the RA-degradative enzyme Cyp26, and that *Cyp26* expression in the neuroepithelium is upregulated by factors derived from the mesoderm and endoderm (Guidato et al., 2003).

Hox genes as determinants of rostrocaudal motoneurone identity

Taken together, the results of our grafting experiments showed that rostrocaudal motoneurone identity and Hox gene expression profile are intimately linked. Nevertheless there were examples to the contrary. For example, r3 grafts in r8a expressed *Hoxa3*, *Hoxb3* and *Hoxd4* but failed to produce hypoglossal SM neurones, which are normally characteristic of neuroepithelium with that Hox 'code'. In addition, somite grafts induced expression of all three Hox genes in r4, but the neurones produced were abducens rather than hypoglossal. Therefore in grafts of r3 to r8a, by the time Hox gene expression is initiated, the time-window for motoneurone specification is already over, whereas for somite grafts, *Hoxa3* has an earlier onset of expression than *Hoxd4*, leading to an abducens phenotype. Another example of the mismatch between Hox expression and motoneurone fate concerns stage 9 r5 grafts to the r3 position; these grafts expressed *Hoxa3* and *Hoxb3* but did not generate SM abducens neurones. In this case, Hox expression was at a lower level than at more caudal axial levels and so levels of Hox protein may not have been high enough to maintain segment identity (Greer et al., 2000).

In a more direct test of the role of Hox genes, we misexpressed *Hoxa3* rostral to its normal expression limit and obtained SM neurone induction in r1-4, which indicates that driving a high level of *Hoxa3* expression could overcome any inherent inhibition of SM neurone production in the rostral hindbrain. Induction of SM neurones by *Hoxa3* could be accomplished in electroporations performed up to stage 15/16. This data is broadly consistent with that from somite grafting experiments in which induction of *Hoxa3* in r4 level occurred approximately 36 hours after grafting, when embryos were approximately stage 15/16, and this was sufficient to induce differentiation of SM neurones with abducens phenotype. *Hoxa3* was found to repress *Irx3* and *Pax6*, and Hb9-expressing SM neurones were found adjacent to, or interspersed with, Chx10-positive cells, which are derived from the Irx3-expressing domain. This suggests that ectopic SM neurones are induced at the expense of presumptive Chx10-positive interneurones. However, no induction of Olig2 was seen in r2-4 of the hindbrain, but it was detected in r1. As Olig2

has been shown to play an important role in SM neurone generation, this implies that *Hoxa3* can function in parallel with, or downstream of, *Olig2* in hindbrain SM neurone differentiation, at least at r2-4 axial levels.

In *Hoxa3* electroporated embryos, SM neurones were present in relatively large numbers in embryos analysed at stage 18, but were present in small numbers at stage 27, when they were restricted to a ventral column on either side of the floor plate and had a phenotype more consistent with abducens identity. These data are thus consistent with Hox3 paralogues being involved with SM specification, and the abducens phenotype in particular. However, the maintenance of these motoneurones following initial induction seems to occur only for more ventrally located cells, and thus may depend on other local factors. In both mouse and chick there are three Hox3 paralogues, *Hoxa3*, *Hoxb3* and *Hoxd3*, which, based on a number of studies, are expressed to a rostral limit at the r4/5 boundary (Capecchi, 1997; Lumsden and Krumlauf, 1996). Although little is known about the early expression pattern of *Hoxd3* in the chick hindbrain, *Hoxa3* and *Hoxb3* are expressed to this rostral limit in the early neural plate (Lumsden and Krumlauf, 1996; Rex and Scotting, 1994). Hence the early expression domains of *Hoxa3* and *Hoxb3* genes coincide with the territory of SM neurone differentiation, making them good candidates for patterning SM neurones. It therefore remains to be determined which Hox genes, and in which combinations, give rise to SM neurones of particular phenotypes. The analysis of various Hox-null mutant mice implicates Hox genes in conferring rostrocaudal identity upon motoneurones (Gavalas et al., 1997; Gavalas et al., 1998; Goddard et al., 1996; Lumsden and Krumlauf, 1996; Studer et al., 1996). In *Hoxa3* mutants, there are defects in the formation of the ganglion of the IX cranial nerve (glossopharyngeal), which may relate to aberrant neural crest migration, and in addition glossopharyngeal (BM/VM) motoneurones in r6 project incorrectly, possibly as a result of the ganglionic defect (Watari et al., 2001). To our knowledge no defects in the abducens or hypoglossal SM neurone populations have been reported in Hox3 paralogue mutants, although neural crest and skeletal patterning are affected (Chisaka and Capecchi, 1991; Condie and Capecchi, 1993). However, because mice mutant for both *Hoxa3* and *Hoxd3* show defects not found in either of the single mutants (Condie and Capecchi, 1993), SM neuronal patterning might require further analysis in these or other double or triple Hox3 mutants.

We thank Drs L. Abbas, J. Briscoe, J. Chilton, J. Ericson and T. Jessell for advice and discussion on the manuscript. We are grateful also to Drs A. Brand, J. Gilthorpe, M. Hofmann, T. Jessell, R. Krumlauf and G. Sauvageau for the gifts of antibodies and cDNA constructs. This work was supported by the Medical Research Council.

REFERENCES

Bell, E., Wingate, R. and Lumsden, A. (1999). Homeotic transformation of rhombomere identity after localized Hoxb1 misexpression. *Science* **284**, 2168-2171.

Berggren, K., McCaffery, P., Drager, U. and Forehand, C. (1999). Differential distribution of retinoic acid synthesis in the chicken embryo as determined by immunolocalization of the retinoic acid synthetic enzyme, RALDH-2. *Dev. Biol.* **210**, 288-304.

Briscoe, J., Sussel, L., Serup, P., Hartigan-O'Connor, D., Jessell, T. M., Rubenstein, J. L. R. and Ericson, J. (1999). Homeobox gene Nkx2.2 and specification of neuronal identity by graded Sonic hedgehog signalling. *Nature* **398**, 622-626.

Briscoe, J., Pierani, A., Jessell, T. and Ericson, J. (2000). A homeodomain protein code specifies progenitor cell identity and neuronal fate in the ventral neural tube. *Cell* **12**, 435-445.

Capecchi, M. (1997). Hox genes and mammalian development. *Cold Spring Harbor Symp. Quant. Biol.* **62**, 273-281.

Chisaka, O. and Capecchi, M. (1991). Regionally restricted developmental defects resulting from targeted disruption of the mouse homeobox gene hox-1.5. *Nature* **350**, 473-479.

Condie, B. and Capecchi, M. (1993). Mice homozygous for a targeted disruption of Hoxd-3 (Hox-4.1) exhibit anterior transformations of the first and second cervical vertebrae, the atlas and the axis. *Development* **119**, 579-595.

Dupé, V. and Lumsden, A. (2001). Hindbrain patterning involves graded responses to retinoic acid signalling. *Development* **128**, 2199-2208.

Ensini, M., Tsuchida, T., Belting, H. and Jessell, T. (1998). The control of rostrocaudal pattern in the developing spinal cord: specification of motor neuron subtype identity is initiated by signal from paraxial mesoderm. *Development* **125**, 969-982.

Ericson, J., Thor, S., Edlund, T., Jessell, T. and Yamada, T. (1992). Early stages of motor neuron differentiation revealed by expression of Homeobox gene Islet-1. *Science* **256**, 1555-1560.

Ericson, J., Morton, S., Kawakami, A., Roelink, H. and Jessell, T. (1996). Two critical periods of Sonic Hedgehog signaling required for the specification of motor neuron identity. *Cell* **87**, 661-673.

Ericson, J., Rashbass, P., Schedl, A., Brenner-Morton, S., Kawakami, A., van Heyningen, V., Jessell, T. M. and Briscoe, J. (1997). Pax6 controls progenitor cell identity and neuronal fate in response to graded Shh signaling. *Cell* **90**, 169-180.

Gale, E., Zile, M. and Maden, M. (1999). Hindbrain respecification in the retinoid-deficient quail. *Mech. Dev.* **89**, 43-54.

Gavalas, A. and Krumlauf, R. (2000). Retinoid signalling and hindbrain patterning. *Curr. Opin. Genet. Dev.* **10**, 380-386.

Gavalas, A., Davenne, M., Lumsden, A., Chambon, P. and Rijli, F. (1997). Role of Hoxa-2 in axon pathfinding and rostral hindbrain patterning. *Development* **124**, 3693-3702.

Gavalas, A., Studer, M., Lumsden, A., Rijli, F., Krumlauf, R. and Chambon, P. (1998). Hoxa1 and Hoxb1 synergize in patterning the hindbrain, cranial nerves and second pharyngeal arch. *Development* **125**, 1123-1136.

Goddard, J., Rossel, M., Manley, N. and Capecchi, M. (1996). Mice with targeted disruption of Hoxb-1 fail to form the motor nucleus of the VIIth nerve. *Development* **122**, 3217-3228.

Gould, A., Itasaki, N. and Krumlauf, R. (1998). Initiation of rhombomeric Hoxb4 expression requires induction by somites and a retinoid pathway. *Neuron* **21**, 39-51.

Grapin-Botton, A., Bonnin, M., McNaughton, L., Krumlauf, R. and Douarin, N. L. (1995). Plasticity of transposed rhombomeres: Hox gene induction is correlated with phenotypic modifications. *Development* **121**, 2707-2721.

Grapin-Botton, A., Bonnin, M. and Douarin, M. L. (1997). Hox gene induction in the neural tube depends on three parameters: competence, signal supply and paralogue group. *Development* **124**, 849-859.

Greer, J., Puetz, J., Thomas, K. and Capecchi, M. (2000). Maintenance of functional equivalence during paralogous Hox gene evolution. *Nature* **403**, 661-665.

Guidato, S., Barrett, C. and Guthrie, S. (2003). Patterning of motor neurons by retinoic acid in the chick embryo hindbrain in vitro. *Mol. Cell. Neurosci.* (in press).

Guthrie, S. and Lumsden, A. (1991). Formation and regeneration of rhombomere boundaries in the developing chick hindbrain. *Development* **112**, 221-229.

Guthrie, S. and Lumsden, A. (1992). Motor neuron pathfinding following rhombomere reversals in the chick embryo hindbrain. *Development* **114**, 663-673.

Guthrie, S., Muchamore, I., Kuroiwa, A., Marshall, H., Krumlauf, R. and Lumsden, A. (1992). Neuroectodermal autonomy of Hox-2.9 expression revealed by rhombomere transpositions. *Nature* **356**, 157-159.

Hacker, A. and Guthrie, S. (1998). A distinct developmental programme for the cranial paraxial mesoderm in the chick embryo. *Development* **125**, 3461-3472.

Hamburger, V. and Hamilton, H. (1951). A series of normal stages in the development of the chick embryo. *J. Morphol.* **88**, 49-92.

Henrique, D., Adam, J., Myat, A., Chitnis, A., Lewis, J. and Ish-Horowicz, D. (1995). Expression of a delta homologue in prospecitve neurons in the chick. *Nature* **375**, 787-790.

Itasaki, N., Sharpe, J., Morrison, A. and Krumlauf, R. (1996). Reprogramming Hox expression in the vertebrate hindbrain: influence of paraxial mesoderm and rhombomere transposition. *Neuron* **16**, 487-500.

Itasaki, N., Bel-Vialar, S. and Krumlauf, R. (1999). 'Shocking' development in chick embryology: electroporation and in ovo gene expression. *Nat. Cell Biol.* **1**, 203-207.

Jessell, T. (2000). Neuronal specification in the spinal cord: inductive signals and transcriptional codes. *Nat. Rev. Genet.* **1**, 20-29.

Jungbluth, S., Bell, E. and Lumsden, A. (1999). Specification of distinct motor neuron identities by the singular activities of individual Hox genes. *Development* **126**, 2751-2758.

Kuratani, S. and Eichele, G. (1993). Rhombomere transplantation repatterns the segmental organization of cranial nerves and reveals cell-autonomous expression of a homeodomain protein. *Development* **117**, 105-117.

Lance-Jones, C. and Landmesser, L. (1980). Motoneurone projection patterns in the chick hind limb following early partial reversals of the spinal cord. *J. Physiol.* **302**, 581-602.

Liu, J., Laufer, E. and Jessell, T. (2001). Assigning the positional identity of spinal motor neurons. Rostrocaudal patterning of Hox-c expression by FGFs, Gdf11, and retinoids. *Neuron* **32**, 997-1012.

Lumsden, A. and Keynes, R. (1989). Segmental patterns of neuronal development in the chick hindbrain. *Nature* **337**, 424-428.

Lumsden, A. and Krumlauf, R. (1996). Patterning the vertebrate neuraxis. *Science* **274**, 1109-1115.

Maden, M. (1996). Retinoids in patterning: chimeras win by a knockout. *Curr. Biol.* **6**, 790-793.

Maden, M. (1999). Heads or tails? Retinoic acid will decide. *BioEssays* **21**, 809-812.

Maden, M., Sonneveld, E., van der Saag, P. T. and Gale, E. (1998). The distribution of endogenous retinoic acid in the chick embryo: implications for developmental mechanisms. *Development* **125**, 4133-4144.

Matise, M. and Lance-Jones, C. (1996). A critical period for the specification of motor pools in the chick lumbosacral spinal cord. *Development* **121**, 659-669.

Momose, T., Tonegawa, A., Takeuchi, J., Ogawa, H., Umesono, K. and Yasuda, K. (1999). Efficient targeting of gene expression in chick embryos by microelectroporation. *Dev. Growth Differ.* **41**, 335-344.

Niederreither, K., Vermot, J., Schuhbaur, B., Chambon, P. and Dolle, P. (2000). Retinoic acid synthesis and hindbrain patterning in the mouse embryo. *Development* **127**, 75-85.

Novitch, B. G., Chen, A. I. and Jessell, T. M. (2001). Coordinate regulation of motor neuron subtype identity and pan-neuronal properties by the bHLH repressor Olig2. *Neuron* **31**, 773-789.

Pfaff, S., Mendelsohn, M., Stewart, C., Edlund, T. and Jessell, T. (1996). Requirement for LIM homeobox gene Isl1 in motor neuron generation reveals a motor neuron-dependent step in interneuron differentiation. *Cell* **84**, 309-320.

Rex, M. and Scotting, P. (1994). Chick HoxB3: deduced amino-acid sequence and embryonic gene expression. *Gene* **149**, 381-382.

Saldivar, J., Krull, C., Krumlauf, R., Ariza-McNaughton, L. and Bronner-Fraser, M. (1996). Rhombomere of origin determines autonomous versus environmentally regulated expression of Hoxa-3 in the avian embryo. *Development* **122**, 895-904.

Sharma, K., Sheng, H., Lettieri, K., Li, H., Karavanov, A., Potter, S., Westphal, H. and Pfaff, S. (1998). LIM homeodomain factors Lhx3 and Lhx4 assign subtype identities for motor neurons. *Cell* **95**, 817-828.

Simon, H. and Lumsden, A. (1993). Rhombomere-specific origin of the contralateral vestibulo-acoustic efferent neurons and their migration across the embryonic midline. *Neuron* **11**, 209-220.

Simon, H., Hornbruch, A. and Lumsden, A. (1995). Independent assignment of antero-posterior and dorso-ventral positional values in the developing chick hindbrain. *Curr. Biol.* **5**, 205-214.

Sockanathan, S. and Jessell, T. (1998). Motor neuron-derived retinoid signaling specifies the subtype identity of spinal motor neurons. *Cell* **94**, 503-514.

Studer, M., Lumsden, A., Ariza-McNaughton, L., Bradley, A. and Krumlauf, R. (1996). Altered segmental identity and abnormal migration of motor neurons in mice lacking Hoxb-1. *Nature* **384**, 630-634.

Swindell, E., Thaller, C., Sockanathan, S., Petkovich, M., Jessell, T. and Eichele, G. (1999). Complementary domains of retinoic acid production and degradation in the early chick embryo. *Dev. Biol.* **216**, 282-296.

Tanabe, Y. and Jessell, T. (1996). Diversity and pattern in the developing spinal cord. *Science* **274**, 1115-1123.

Tanabe, Y., William, C. and Jessell, T. (1998). Specification of motor neuron identity by the MNR2 homeodomain protein. *Cell* **95**, 67-80.

Tsuchida, T., Ensini, M., Morton, S., Baldassare, M., Edlund, T., Jessell, T. and Pfaff, S. (1994). Topographic organization of embryonic motor neurons defined by expression of LIM homeobox genes. *Cell* **79**, 957-970.

Vaage, S. (1969). The segmentation of the primitive neural tube in chick embryos (*Gallus domesticus*). A morphological, histochemical and autoradiographical investigation. *Ergeb. Anat. Entwicklungsgesch* **41**, 3-87.

Varela-Echavarría, A., Pfaff, S. and Guthrie, S. (1996). Differential expression of LIM homeobox genes among motor neuron subpopulations in the developing chick brain stem. *Mol. Cell. Neurosci.* **8**, 242-257.

Wahl, C., Noden, D. and Baker, R. (1994). Developmental relations between sixth nerve motor neurons and their targets in the chick embryo. *Dev. Dyn.* **201**, 191-202.

Watari, N., Kameda, Y., Takeichi, M. and Chisaka, O. (2001). Hoxa3 regulates integration of glossopharyngeal nerve precursor cells. *Dev. Biol.* **240**, 15-31.